

## A simple method of labeling amyloid $\beta$ with quantum dots and ingestion of the labeled amyloid $\beta$ by astrocytes

This article has been downloaded from IOPscience. Please scroll down to see the full text article.

2013 Nanotechnology 24 035101

(<http://iopscience.iop.org/0957-4484/24/3/035101>)

View [the table of contents for this issue](#), or go to the [journal homepage](#) for more

Download details:

IP Address: 138.26.31.3

The article was downloaded on 13/03/2013 at 08:17

Please note that [terms and conditions apply](#).

# A simple method of labeling amyloid $\beta$ with quantum dots and ingestion of the labeled amyloid $\beta$ by astrocytes

Jing Zhang<sup>1</sup>, Xing Jia<sup>1</sup>, Hong Qing and Hai-Yan Xie

School of Life Science, Beijing Institute of Technology, Beijing 100081, People's Republic of China

E-mail: [hyanxie@bit.edu.cn](mailto:hyanxie@bit.edu.cn)

Received 20 September 2012, in final form 26 October 2012

Published 21 December 2012

Online at [stacks.iop.org/Nano/24/035101](http://stacks.iop.org/Nano/24/035101)

## Abstract

Steady labeling of amyloid beta ( $A\beta$ ) is crucial for studying the ingestion and degradation of  $A\beta$  by astrocytes and unraveling a relevant regulation mechanism. Quantum dots (QDs) are an optimum labeling reagent for this because of their strong and steady fluorescence properties. In this paper,  $A\beta$  was labeled with QDs by a simple mixed incubation strategy, with a QD labeled  $A\beta$  complex (QDs- $A\beta$ ) being obtained. In the complex, QDs efficiently restrained the formation of  $\beta$ -folding and fibrils of  $A\beta$ , while the graininess, dispersivity and fluorescence properties of the QDs hardly changed. The fluorescence microscopy imaging results showed that the astrocytes could ingest the QDs- $A\beta$ . The QDs and  $A\beta$  did not separate from each other during the ingestion process, and the  $A\beta$  could be degraded subsequently.

(Some figures may appear in colour only in the online journal)

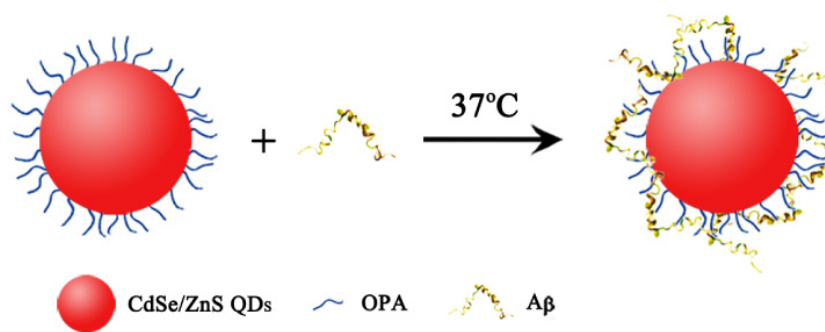
## 1. Introduction

Alzheimer's disease (AD) is a neurodegenerative disorder characterized by a progressive cognitive decline [1]. The driving force of AD is an imbalance between the production and the clearance of amyloid beta ( $A\beta$ ), which results in the extracellular deposition of  $A\beta$ . The deposition of aggregated  $A\beta$  induces a series of complex responses, among which the final is loss of neurons, formation of intra-neuronal neurofibrillary tangles, and extracellular plaques composed primarily of deposits of  $A\beta$  aggregates [2, 3]. So lessening or inhibiting the deposition of  $A\beta$  and increasing the ability to clear  $A\beta$  in the brain could reduce or prevent the lesions of AD. Clearance of  $A\beta$  as a remedy for AD is a major target in on-going clinical trials. Astrocytes, the major glial cell type in the central nervous system (CNS), are considered to be the main immune effector cells capable of ingesting and degrading  $A\beta$  [4–10]. But the related mechanism is not so clear. Many research results cannot confirm each other, and some are contradictory. One of the reasons for this situation is the lack of an efficient method for  $A\beta$  labeling, and it

is impossible to track in real-time the dynamic process and transformation of  $A\beta$ .

Nanoparticles possess large surface to volume ratios, surface energies, and their surface tensions increase with decrease in the particle diameters [11]. They show some special characteristics, such as small size effect and a surface–interface effect. Moreover, nanoparticles are of a similar size to macromolecules. The interaction between them may have an important influence on the structure of the macromolecules. Some research results have proved that nanoparticles can affect the congregation of  $A\beta$  [12–21]. PEGylated phospholipid nanomicelles could interact with  $A\beta_{42}$  and evidently reduce its aggregation potential and nerve toxicity [12]. Sulfonated and sulfated polystyrenes affected the conformation of  $A\beta$  inducing a disordered state [13]. Then, oligomerization was delayed and cytotoxicity reduced. Fullerene was found to significantly inhibit the amyloid formation of  $A\beta_{40}$  by specifically binding to its central hydrophobic motif, KLVFF [14]. Fluorinated nanoparticles were shown to induce a helical structure in  $A\beta_{40}$ , leading to no peptide aggregation or  $A\beta$  fibrillogenesis [15]. Copolymeric NiPAM:BAM nanoparticles of varying hydrophobicity were found to inhibit  $A\beta$

<sup>1</sup> Contributed equally.



**Scheme 1.** The preparation of the QD labeled A $\beta$  (QDs-A $\beta$ ).

fibrillation by mainly influencing the nucleation step instead of the elongation step [16].

In contrast to the above results, some reports indicated that nanoparticles promoted the fibrillation process of A $\beta$  [22–25]. This might be attributed to a condensation-ordering mechanism [23] and some other characteristics of nanoparticles, such as surface charge, hydrophobicity, hydrodynamic size and particle stability against aggregation [22].

As a kind of new type of fluorescence labeling material, quantum dots (QDs) have unique advantages in real-time dynamic imaging research [26]. By taking advantage of this, Tokuraku *et al* covalently conjugated cysteine modified A $\beta$  with QDs (QDs-A $\beta$ ), and studied the dynamic process of A $\beta$  fibrillation *in vitro*. When coincubated with microglial cells, QDs-A $\beta$  could be taken up by the microglial cells as normal and appeared in lysosomes in 24 h [27]. By using this QDs-A $\beta$ , they also studied the effect of an inhibitory drug on the coaggregates of A $\beta$  [28]. Xiao *et al* reported that there was a significant change in the morphology of fibrils and the fibrillation process when A $\beta$  was mixed or conjugated to the QDs [29]. It maybe possible that QDs-A $\beta$  can be used as a diagnostic and therapeutic probe, if something can be designed that is able to cross the blood–brain barrier (BBB) and the QD safety considerations can be satisfied [30–32].

In this paper, A $\beta$  was labeled with QDs (QDs-A $\beta$ ) by a simple mixed incubation strategy through which A $\beta$  became wrapped on the surface of QDs (scheme 1). QDs inhibited the formation of  $\beta$ -folding, interdicted the fibrillation process of A $\beta$ , and did not evidently influence the nerve toxicity of A $\beta$ . The QDs-A $\beta$  still had perfect graininess, dispersivity and fluorescence properties. When coincubated with astrocytes, the QDs-A $\beta$  could be ingested. QDs and A $\beta$  did not separate from each other during the ingestion process, and the A $\beta$  was degraded in 24 h, indicating that labeling of A $\beta$  with QDs did not affect the uptake and degradation of astrocytes for A $\beta$ . This provided a possible new method for visualizing and studying the process of astrocytes ingesting and eliminating A $\beta$ .

## 2. Experimental section

### 2.1. Materials and reagents

Carboxyl functionalized CdSe/ZnS QDs605 was purchased from Jiayuan Quantum Dots Co. Ltd (Wuhan, China). A $\beta$

protein was purchased from American Peptide Co. Ltd (USA). The SH-SY5Y cell line was kindly provided by the University of British Columbia (CAN). Sprague Dawley neonate rats were purchased from Fangyuanyuan Nursery (Beijing, China). 1,1,1,3,3,3-Hexafluoro-2-propanol (HFIP) was from Bailingwei Co. Ltd (Beijing, China). Dulbecco's modified Eagle's medium with high glucose (DMEM) and fetal bovine serum (FBS) were all bought from Gibco Co. Ltd (USA). All the cell culture materials were from Corning Co. Ltd (USA). 3-(4,5-Dimethylthiazol-2-yl)-2,5-diphenyl tetrazolium bromide (MTT) and dimethyl sulfoxide (DMSO) were from Amresco Co. Ltd (Germany). Hoechst 33342 and poly-L-lysine were from Sigma Co. Ltd (USA). The DAB Kit was from Kangwei Tech Co. Ltd (Beijing, China). BAM-10 monoclonal antibody was from Sigma Co. Ltd (USA) and 4G8 monoclonal antibody was from Covance Co. Ltd (USA). Mouse anti-glia fibrillary acidic protein (GFAP) was from Cell Signaling (USA). Fluorescein isothiocyanate (FITC)-conjugated goat anti-mouse IgG, Cy3-conjugated goat anti-mouse IgG and horseradish peroxidase (HRP)-conjugated goat anti-mouse IgG were from ProteinTech Co. Ltd (USA). All other chemical reagents were all purchased from Beijing Chemical Co. Ltd (Beijing, China).

### 2.2. Preparation of monomer A $\beta$ peptide

A $\beta$  protein was conserved at  $-20^{\circ}\text{C}$  before use. After being equilibrated at room temperature for 30 min, the A $\beta$  protein powder was dissolved in HFIP at a concentration of  $1\text{ mg ml}^{-1}$ . The solution was incubated at room temperature for 1 h followed by sonication for 10 min with monomer A $\beta$  peptide obtained. Then the aliquot was slowly dried under a  $\text{N}_2$  atmosphere at  $4^{\circ}\text{C}$  and stored at  $-20^{\circ}\text{C}$ .

### 2.3. Immuno-dot blot assay

HFIP-treated A $\beta$  peptides were dispersed in phosphate-buffered saline (PBS; 0.01 M, 0.15 M NaCl, pH = 7.2) with a final concentration of  $100\text{ }\mu\text{M}$ . QDs-A $\beta$  samples at different CdSe/ZnS QDs to A $\beta$  concentration ratios were prepared by mixing a certain amount of QDs and A $\beta$ , then incubating for 1–7 days at  $37^{\circ}\text{C}$ . A  $2\text{ }\mu\text{l}$  aliquot of each sample was hand-spotted onto a prepared nitrocellulose (NC) membrane. The NC membrane with samples was dried at

37 °C for 30 min and blocked with 10% non-fat milk in PBST (0.01 M PBS with 0.15 M NaCl and 0.1% Tween 20) for 1 h at room temperature. Then it was washed three times and incubated with BAM-10 diluted 1:1500 in PBST with 3% bovine serum albumin (BSA) for 1 h at room temperature. After primary immune-reaction, the membrane was incubated with HRP-conjugated goat anti-mouse IgG (diluted 1:5000 in PBST with 3% BSA) for 1 h at room temperature. Then the membrane was washed again and a final detection was performed with a DAB Kit.

#### 2.4. Circular dichroism (CD) spectroscopy

HFIP-treated A $\beta$  peptides were re-dispersed in PBS at a final concentration of 50  $\mu$ M (or 20  $\mu$ M) in the absence or presence of 200 nM QDs. After having been incubated at 37 °C for different times, the secondary structure changes of A $\beta$  were measured on a J-715-150L spectropolarimeter (Jasco Co., Japan). Spectra were recorded in the range of 250–190 nm for  $\beta$ -sheet structures exhibiting two characteristic ellipticities of 215 nm (min) and 196 nm (max). Each spectrum was an average of three scans at a speed of 50 nm min<sup>-1</sup> with a resolution of 0.2 nm.

#### 2.5. Atomic force microscopy

Pre-incubated QDs-A $\beta$ , QDs or A $\beta$  at certain concentrations (A $\beta$ , 20  $\mu$ M; QDs, 200 nM) were respectively deposited onto pre-cleaned silicon slices and incubated for 15 min. After having been washed three times with deionized water and dried at room temperature, the slices were glued to a magnetic pallet and imaged by a CP-II type atomic force microscope (Veeco, USA).

#### 2.6. Transmission electron microscopy

Pre-incubated QDs-A $\beta$ , QDs or A $\beta$  at certain concentrations (A $\beta$ , 20  $\mu$ M; QDs, 200 nM) were respectively spread on clean carbon-coated Ni grids for 2 min and negatively stained with 2% uranium acetate for 30 s. Measurements were taken under a JEM-1400 transmission electron microscope (JEDL, Japan) with an acceleration voltage of 80 kV.

#### 2.7. MTT assay

SH-SY5Y cells were pre-cultured in 96 wells at a density of  $5 \times 10^3$  ml<sup>-1</sup> 24 h before use. Then the culture medium was discarded and pre-incubated QDs-A $\beta$ , QDs or A $\beta$  dispersed in fresh culture medium samples at certain concentrations were added. After 24 h incubation under 5% CO<sub>2</sub> at 37 °C, the cells were washed three times. Then 180  $\mu$ l of serum-free fresh medium supplemented with 20  $\mu$ l MTT solution (5 mg ml<sup>-1</sup>) was added into each well and incubated at 37 °C for 4 h. All solutions were discarded and 200  $\mu$ l DMSO was added into each well to dissolve the dark pellet which was formed by the mitochondrial reductase of living cells. The 520 nm absorbance was measured by a Mutiskan Ascent microplate reader (Thermo, USA) and cell survival rates were calculated. Data were represented as mean  $\pm$  standard deviation (SD) for three independent determinations.

#### 2.8. Astrocyte culture

Primary astrocytes were isolated from neonatal rat brain cortex. Cerebra cortices were transferred into D-Hanks buffer and clipped into pieces, followed by 0.25% trypsin-EDTA digestion for 30 min. Medium with 10% FBS was added to stop the digestion and the suspension was centrifuged at 3000 rpm to get cell precipitates. The precipitated cells resuspended in medium were filtered through a 400 mesh cloth membrane and transferred into a 75 cm<sup>2</sup> flask. Cell cultures were incubated in 5% CO<sub>2</sub> at 37 °C for 1 h to get rid of fibrocytes. Then cells in supernatant were recollected through centrifugation and plated into poly-L-lysine coated flasks with DMEM medium containing 10% FBS. The primary astrocytes were cultured in 5% CO<sub>2</sub> at 37 °C for a week. Before the experiments the astrocytes were shaken at 240 rpm for 18 h to remove microglia and oligodendrocytes. Mouse anti-GFAP was used to determine the purity of astrocytes.

#### 2.9. Ingestion of QDs-A $\beta$ /A $\beta$ by astrocytes

Purified astrocytes were seeded into poly-L-lysine coated glass slides and cultured for 24 h. QDs-A $\beta$  or A $\beta$  at certain concentrations were added to incubate with the astrocytes for a certain time. Then the cells were washed three times and fixed with 4% paraformaldehyde for 30 min at room temperature. The fixed cells were first permeabilized in 0.3% Tween 20 for 15 min and then blocked by 5% BSA in PBS for 1 h. Primary antibody was diluted by PBS with 5% BSA in certain ratios and added to incubate with the cells for 1 h at room temperature. After having been washed with PBS three times, the cells were allowed to incubate with diluted fluor-labeled secondary antibody for 1 h. Nuclei were stained by Hoechst 33342 for 15 min. Finally the cells were visualized under a TCS SP5 laser confocal microscope (Leica, Germany) (excitation, 488 nm for QDs and FITC, 405 nm for Hoechst 33342; emission wavelength coverage, 510–540 nm for FITC, 590–610 nm for QDs, 450–480 nm for Hoechst 33342.)

### 3. Results and discussion

#### 3.1. Effects of QDs on A $\beta$ aggregation detected by immuno-dot blot assay

A monoclonal antibody, BAM-10, was used to perform the immuno-dot blot assay, which could specifically interact with the amino acid residues 1–12 of the A $\beta$  sequence. The reactivity of BAM-10 diminished as aggregation proceeded because the recognition location was gradually concealed in this process. The effects of CdSe/ZnS QDs on aggregation of A $\beta$  could accordingly be estimated.

As can be seen from the immuno-dot blot assay results (figure 1), BAM-10 reactivity diminished as aggregation proceeded with increasing time, temperature and peptide concentration. In detail, BAM-10 reactivity was still detectable after A $\beta$  at a concentration of 20  $\mu$ M had been incubated for 7 days at 4 °C. However, it started to fade after

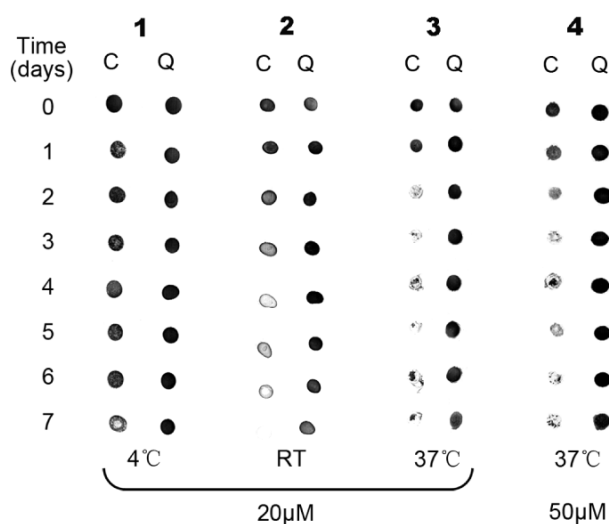


**Figure 1.** Immuno-dot blot assay of A $\beta$  aggregation. 1–3, A $\beta$  solutions (20  $\mu$ M) were incubated for 0–7 days at different temperatures (4  $^{\circ}$ C, room temperature, 37  $^{\circ}$ C) with 200 nM QDs (Q) or without QDs (C). 4, A $\beta$  solutions (50  $\mu$ M) were incubated for 0–7 days at 37  $^{\circ}$ C with 200 nM QDs (Q) or without QDs (C).

4 days at room temperature and was rendered undetectable only after 2 days at 37  $^{\circ}$ C, indicating extensive aggregation. But the BAM-10 immuno-reactivity was always detectable in the presence of 200 nM QDs, even after having been coincubated for 7 days at 37  $^{\circ}$ C, demonstrating efficient inhibition of A $\beta$  fibrillation. Similar results were obtained when the concentration of A $\beta$  was increased to 50  $\mu$ M (figure 1).

### 3.2. Effects of QDs on the secondary structure of A $\beta$

CD spectroscopy was used to assay if the formation of  $\beta$ -folding during the aggregation process was affected by the addition of QDs. A $\beta$  was allowed to incubate with QDs and detected at 0, 2 and 4 days. A $\beta$  at the same concentrations and incubation times was used as a control (figure 2).

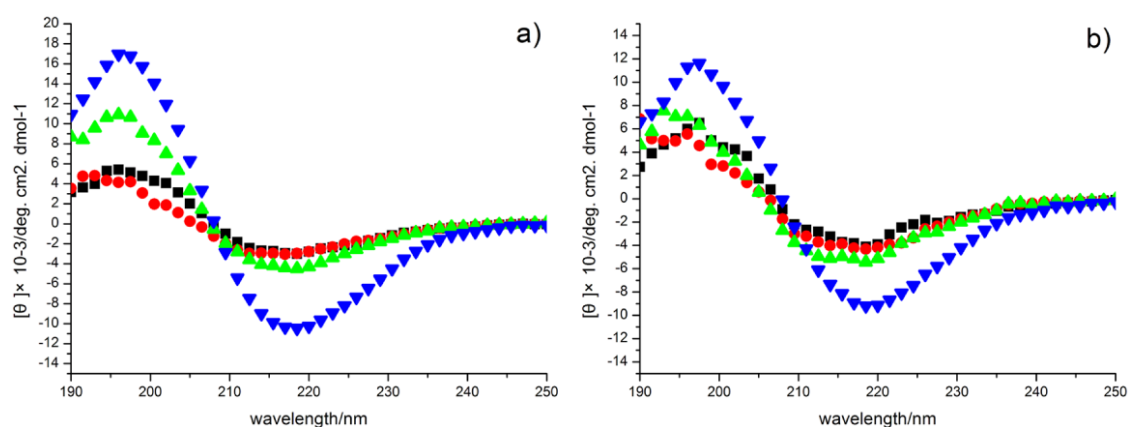


**Figure 2.** CD spectra of A $\beta$  peptides incubated for different times with or without QDs. (a) 20  $\mu$ M A $\beta$  incubated with 200 nM QDs for 0 days (■), 2 days (●), 4 days (▲) or without QDs for 4 days (▼) at 37  $^{\circ}$ C. (b) 50  $\mu$ M A $\beta$  incubated with 200 nM QDs for 0 days (■), 2 days (●), 4 days (▲) or without QDs for 4 days (▼) at 37  $^{\circ}$ C.

It was found that the  $\beta$ -folding of A $\beta$  was evidently inhibited in the presence of QDs (figure 2). When the ratio of  $C_{A\beta}$  to  $C_{QDs}$  decreased to 100:1, there was still no distinct  $\beta$ -folding formation after having been coincubated for 4 days. When the ratio of  $C_{A\beta}$  to  $C_{QDs}$  was 250:1, the signal of  $\beta$ -folding appeared after 4 days' coincubation, but it was obviously lower than that of A $\beta$ . The immuno-dot blot assay and CD spectroscopy assay results were consistent with each other. It was reliably shown that the addition of QDs could inhibit the fibrillation process of A $\beta$  by decreasing  $\beta$ -fold formation and keeping it in a low aggregation situation. This might be because the surface to volume ratio of QDs was very large and A $\beta$  could wrap onto the QD surface as an extending structure. At the same time, the effective concentration of A $\beta$  in solution decreased, and the aggregation of A $\beta$  consequently decreased. Based on the above results, the QDs-A $\beta$  was prepared by coincubating A $\beta$  with QDs ( $C_{A\beta}:C_{QDs} = 100:1$ ) at 37  $^{\circ}$ C for 2 days in the following experiments.

### 3.3. Effects of A $\beta$ on the graininess of QDs

QDs dispersed in solution with uniform steady graininess. In the QDs-A $\beta$  system, however, QDs could inhibit the aggregation of A $\beta$  as mentioned above; but also A $\beta$  might affect the dispersivity of QDs. So we characterized the graininess of QDs-A $\beta$  by AFM and TEM.

AFM detection depends on the repulsive force between the atoms on the tip and surface atoms on the specimen. So AFM results mainly show the surface morphology of specimens. As can be seen in figure 3, QDs have perfect graininess and uniform size with a diameter of about 30 nm. Compared with QDs, the size of QDs-A $\beta$  increased a little and became less uniform. Some of the particles were even relatively big. But, on the whole, QDs-A $\beta$  kept their good graininess. It was not difficult to find that the adsorption capacity of silicon slices for QDs-A $\beta$  was evidently stronger than that for QDs, which might be due to the stronger adsorption interaction between A $\beta$  and silicon slices.

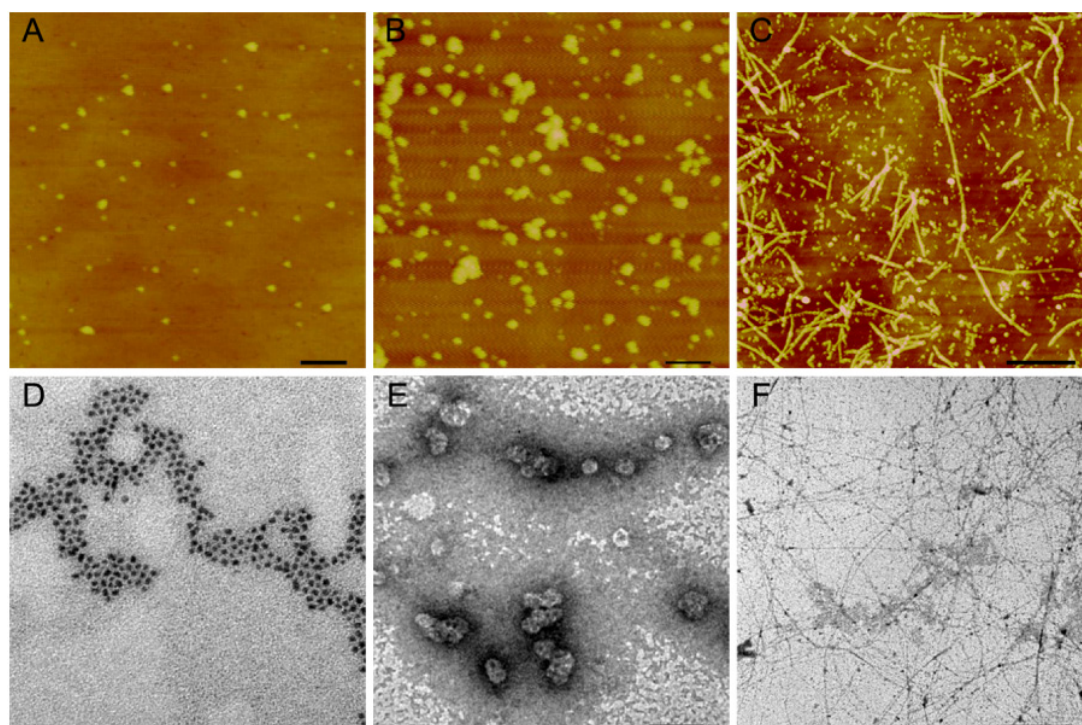


**Figure 3.** Detection of the graininess of QDs-A $\beta$ . A–C, QDs, QDs-A $\beta$  and A $\beta$  detected by AFM; D–F, QDs, QDs-A $\beta$  and A $\beta$  detected by TEM with negative staining. Scale bar for each image: A, B (200 nm); D, E (50 nm); C, F (5  $\mu$ m).

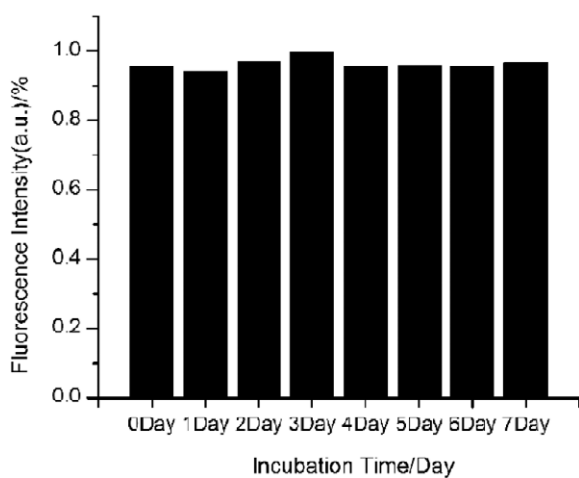


**Figure 4.** Fluorescence intensity of QDs-A $\beta$  incubated for different times (20  $\mu$ M A $\beta$  was coincubated with 200 nM QDs for 7 days at 37  $^{\circ}$ C and the solution was detected every 24 h). The fluorescence intensity of QDs-A $\beta$  was normalized to a percentage of the same concentration of the QDs. A FluoroMax-4 spectrofluorometer (Horiba Jobin Yvon, USA) was used and the excitation wavelength was 488 nm.

The TEM imaging results also showed that QDs were of uniform graininess and well dispersed (figure 3(D)), and there were small-scale aggregations of QDs in QDs-A $\beta$ . But QDs could still be distinguished in these aggregations. The big particles in the QDs-A $\beta$  might be because A $\beta$  wrapped onto different QD particles or part of A $\beta$  aggregated in a short distance. But they were not aggregations of QDs themselves. When A $\beta$  at the same concentration was incubated at 37  $^{\circ}$ C

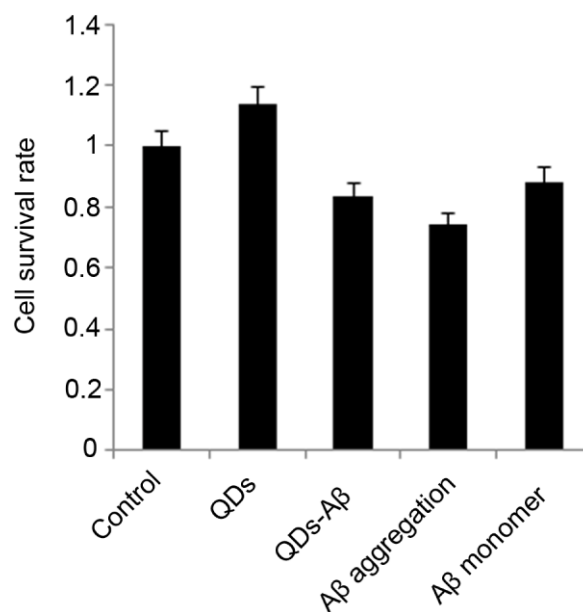


**Figure 5.** Effects of QDs on A $\beta$  cytotoxicity ( $n = 3, p < 0.05$ ).

for 2 days, a great number of visible fibers formed. This hardly happened in all QDs-A $\beta$  samples. This indicated that QDs inhibited the fibrillation of A $\beta$  while keeping their own dispersivity, which was consistent with the results of immuno-dot blot assay and CD spectroscopy assays.

#### 3.4. Effects of A $\beta$ on the fluorescence of QDs

The spectral results showed that the fluorescence properties of QDs hardly changed after the addition of A $\beta$ , even if they had

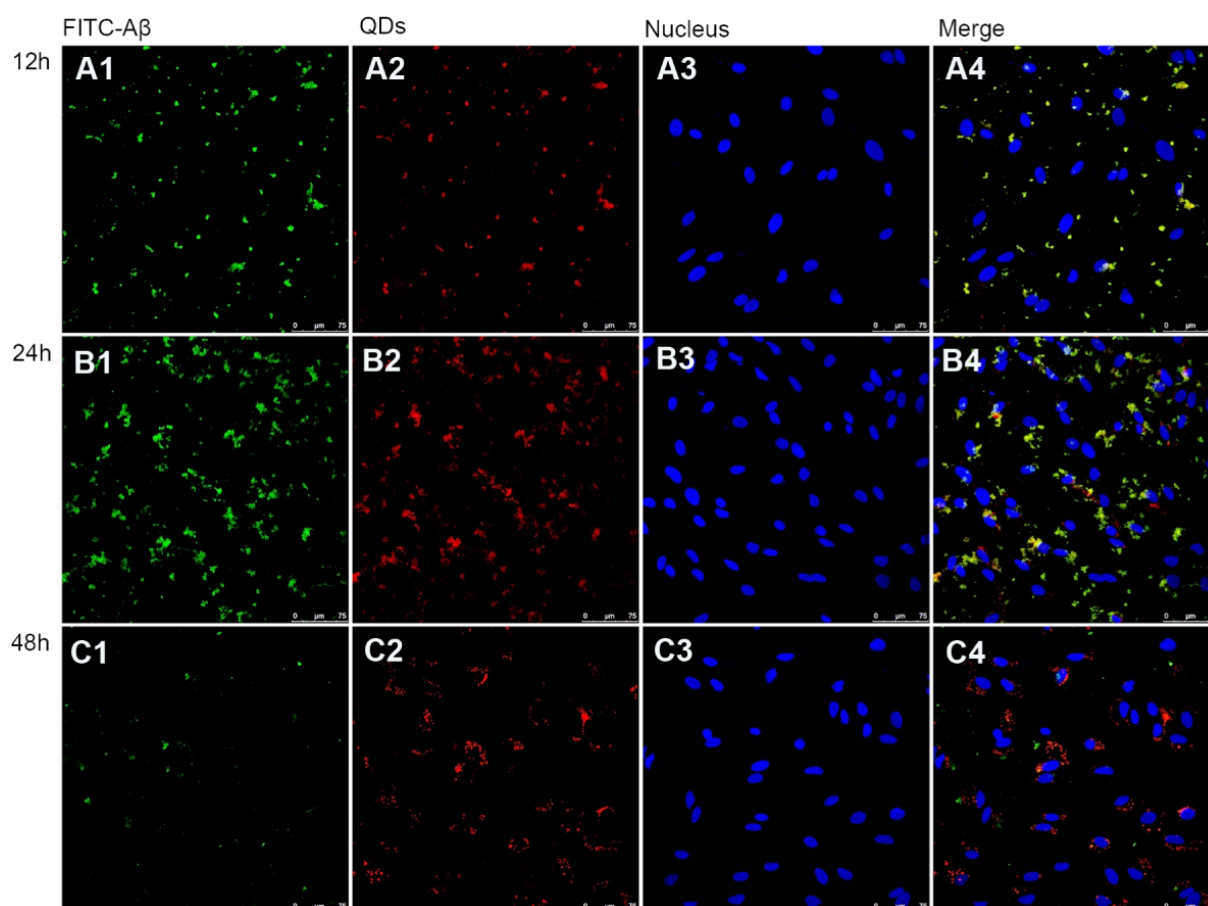


**Figure 6.** Fluorescence images of the dynamic internalization of QDs-A $\beta$  by astrocytes for certain times. A1–4, 12 h; B1–4, 24 h; C1–4, 48 h. Green fluorescence for FITC-labeled A $\beta$ . Red fluorescence for QDs. Blue fluorescence for nucleus stained by Hoechst 33342. Scale bar is 75  $\mu$ m.

been coincubated for 7 days (figure 4). This was no surprise to us since A $\beta$  only wrapped onto the surface of the QDs by interacting with the modified molecules on the QDs. They did not influence the interaction between the modifying molecules and QDs, let alone the surface structure of the QDs.

### 3.5. Effects of QDs on the nerve toxicity of A $\beta$

It was reported that there are three forms for A $\beta$  in the brain, namely monomers, oligomers and fibers. The toxicity of oligomers is stronger than that of monomers and fibers. It is a serious problem that the oligomers cannot be phagocytized by microglia [27]. As mentioned above, QDs could inhibit the fibrillation of A $\beta$ . But it is still unclear if QDs influence the formation of oligomers and the toxicity of A $\beta$ . So the toxicity of A $\beta$  in QDs-A $\beta$  was another important problem in evaluating if QDs-A $\beta$  is suitable for cell research.

As can be seen from the MTT assay results (figure 5), QDs did not influence the activity of cells. The toxicity of the monomers of A $\beta$  was less than the A $\beta$  aggregation formed by incubating at 37°C for 2 days. QDs-A $\beta$  prepared by coincubating QDs with A $\beta$  for 2 days had less influence on cell viability than A $\beta$  aggregating in the same conditions. Integrating the CD spectroscopy assay results, it could be

speculated that QDs inhibited the  $\beta$ -fold formation of A $\beta$  to some extent when QDs-A $\beta$  came into being. The aggregation and toxicity of A $\beta$  decreased accordingly.

### 3.6. The ingestion of QDs-A $\beta$ by astrocytes

To demonstrate if QDs are suitable as a label for tracking A $\beta$ , QDs-A $\beta$  was allowed to incubate with astrocytes. The ingestion and degradation of QDs-A $\beta$  by astrocytes was studied (figure 6). Because BAM-10 could only recognize the monomers or oligomers of A $\beta$  which could expose the epitope (amino acids 1–12 of the A $\beta$  sequence), and could not recognize the aggregations formed after 2 days' coincubation. Thereby, 4G8 monoclonal antibody was used in cell immuno-labeling. It could recognize monomers, oligomers and big aggregations without exception, because its epitope (amino acids 17–24 of the A $\beta$  sequence) was not concealed during the folding process of A $\beta$  [33].

The results showed that part of QDs-A $\beta$  was ingested into astrocytes when they had incubated for 12 h, and QDs did not separate from A $\beta$  in that time. At 24 h, both signals of A $\beta$  and QDs were obvious and colocalized well. A few signals of QDs presented around the nucleolus alone, which might be

due to part of the QDs- $A\beta$  ingested into the astrocytes earlier being degraded at that time. When the incubation had lasted for 48 h,  $A\beta$  in cells was widely degraded, indicating QDs could be used as fluorescence labeling reagents for tracking the endocytosis and degradation of  $A\beta$ .

#### 4. Conclusions

In this paper, we introduced a simple mixed incubation method to adsorb  $A\beta$  onto QD surfaces and realized the integration of  $A\beta$  and QDs (QDs- $A\beta$ ). In the QDs- $A\beta$  complex, QDs could decrease the  $\beta$ -folding and interdicted the fibrillation process of  $A\beta$ , but did not increase its toxicity. QDs- $A\beta$  was still of good graininess and dispersivity, and the fluorescence properties of QDs were unchanged. QDs- $A\beta$  could be ingested by astrocytes. QDs and  $A\beta$  did not separate from each other during the endocytosis process, and  $A\beta$  was almost degraded after coincubation with astrocytes for 48 h. This indicated that after the integration, QDs did not influence the degradation and elimination capacity of astrocytes for  $A\beta$ .

#### Acknowledgments

This work was supported by the National Basic Research Program of China (973 Program, no. 2011CB933600), the National Natural Science Foundation of China (no. 20975013) and the Program for New Century Excellent Talents in University (no. NCET-08-0046).

#### References

- [1] Minati L, Edginton T, Bruzzone M G and Giaccone G 2009 Reviews: current concepts in Alzheimer's disease: a multidisciplinary review *Am. J. Alzheimer's Dis.* **24** 95–121
- [2] Selkoe D J 2001 Alzheimer's disease: genes, proteins, and therapy *Physiol. Rev.* **81** 741–66
- [3] Dickson D W 1998 Neuropathological diagnosis of Alzheimer's disease: a perspective from longitudinal clinicopathological studies *Neurobiol. Aging* **18** S21–6
- [4] LaDu M J, Shah J A, Reardon C A, Getz G S, Bu G, Hu J R, Guo L and Van Eldik L J 2000 Apolipoprotein E receptors mediate the effects of  $\beta$ -amyloid on astrocyte cultures *J. Biol. Chem.* **275** 33974–80
- [5] Nielsen H M, Mulder S D, Beliën J A M, Musters R J P, Eikelenboom P and Veerhuis R 2010 Astrocytic  $A\beta$ 1–42 uptake is determined by  $A\beta$ -aggregation state and the presence of amyloid-associated proteins *Glia* **58** 1235–46
- [6] Wyss-Coray T, Loike J D, Brionne T C, Lu E, Anankov R, Yan F R, Silverstein S C and Husemann J 2003 Adult mouse astrocytes degrade amyloid- $\beta$  *in vitro* and *in situ* *Nature Med.* **9** 453–7
- [7] Brandenburg L O, Konrad M, Wruck C, Koch T, Pufe T and Lucius R 2008 Involvement of formyl-peptide-receptor-like-1 and phospholipase D in the internalization and signal transduction of amyloid beta 1–42 in glial cells *Neuroscience* **156** 266–76
- [8] Okabayashi S and Kimura N 2008 Leucine-rich glioma inactivated 3 is involved in amyloid  $\beta$  peptide uptake by astrocytes and endocytosis itself *Neuroreport* **19** 1175–9
- [9] Nagele R G, D'Andrea M R, Lee H, Venkataraman V and Wang H Y 2003 Astrocytes accumulate  $A\beta$  42 and give rise to astrocytic amyloid plaques in Alzheimer disease brains *Brain Res.* **971** 197–209
- [10] Nielsen H M, Veerhuis R, Holmqvist B and Janciauskiene S 2009 Binding and uptake of  $A\beta$  1–42 by primary human astrocytes *in vitro* *Glia* **57** 978–88
- [11] Burda C, Chen X B, Narayanan R and El-Sayed M A 2005 Chemistry and properties of nanocrystals of different shapes *Chem. Rev.* **105** 1025–102
- [12] Pai A S, Rubinstein I and Onyukel H 2006 PEGylated phospholipid nanomicelles interact with  $\beta$ -amyloid (1–42) and mitigate its  $\beta$ -sheet formation, aggregation and neurotoxicity *in vitro* *Peptides* **27** 2858–66
- [13] Saraiva A M, Cardoso I, Saraiva M J, Tauer K, Pereira M C, Coelho M A N, Mohwald H and Brezesinski G 2010 Randomization of amyloid- $\beta$ -peptide (1–42) conformation by sulfonated and sulfated nanoparticles reduces aggregation and cytotoxicity *Macromol. Biosci.* **10** 1152–63
- [14] Kim J E and Lee M 2003 Fullerene inhibits  $\beta$ -amyloid peptide aggregation *Biochem. Biophys. Res. Commun.* **303** 576–9
- [15] Rocha S, Thunemann A F, Pereira M C, Coelho M, Mohwald H and Brezesinski G 2008 Influence of fluorinated and hydrogenated nanoparticles on the structure and fibrillogenesis of amyloid beta-peptide *Biophys. Chem.* **137** 35–42
- [16] Cabaleiro-Lago C, Quinlan-Pluck F, Lynch I, Lindman S, Minogue A M, Thulin E, Walsh D M, Dawson K A and Linse S 2008 Inhibition of amyloid  $\beta$  protein fibrillation by polymeric nanoparticles *J. Am. Chem. Soc.* **130** 15437–43
- [17] Keisuke I, Takuma O, Shin-ichi S, Kazunari A and Katsumi M 2006 Inhibition of the formation of amyloid  $\beta$ -protein fibrils using biocompatible nanogels as artificial chaperones *FEBS Lett.* **580** 6587–95
- [18] Garima T, Miodrag M, Yuehai Y, Wenzhi L, Dania M, Silvia G, Hongzhou Z and Roger M L 2011 Conjugated quantum dots inhibit the amyloid  $\beta$  (1–42) fibrillation process *Int. J. Alzheimer's Dis.* **2011** 502386
- [19] Hadas S, Gilead S and Shlomo M 2011 Acceleration and inhibition of amyloid- $\beta$  fibril formation by peptide-conjugated fluorescent-maghemite nanoparticles *J. Nanopart. Res.* **13** 3521–34
- [20] Sabrina D, Valeria C, Ian W H and Sébastien P 2012 Altering peptide fibrillization by polymer conjugation *Biomacromolecules* **13** 2739–47
- [21] Chan H M, Xiao L, Yeung K M, Ho S L, Zhao D, Chan W H and Li H W 2012 Effect of surface-functionalized nanoparticles on the elongation phase of beta-amyloid (1–40) fibrillogenesis *Biomaterials* **33** 4443–50
- [22] Vicki L C and Kristen M K 2007 Nanoparticles as catalysts for protein fibrillation *Proc. Natl Acad. Sci. USA* **104** 8679–80
- [23] Stefan A, Antonio T and Michele V 2009 A condensation-ordering mechanism in nanoparticle-catalyzed peptide aggregation *PLoS Comput. Biol.* **5** e1000458
- [24] Linse S, Cabaleiro-Lago C, Xue W F, Lynch I, Lindman S, Thulin E, Radford S E and Dawson K A 2007 Nucleation of protein fibrillation by nanoparticles *Proc. Natl Acad. Sci. USA* **104** 8691–6
- [25] Wu W H, Sun X, Yu Y P, Hu J, Zhao L, Liu Q, Zhao Y F and Li Y M 2008  $TiO_2$  nanoparticles promote  $\beta$ -amyloid fibrillation *in vitro* *Biochem. Biophys. Res. Commun.* **373** 315–8
- [26] Dahan M, Levi S, Luccardini C, Rostaing P, Riveau B and Triller A 2003 Diffusion dynamics of glycine receptors revealed by single-quantum dot tracking *Science* **302** 442–5
- [27] Tokuraku K, Marquardt M and Ikezu T 2009 Real-time imaging and quantification of amyloid- $\beta$  peptide aggregates by novel quantum-dot nanoprobe *PLoS One* **4** e8492
- [28] Tokuraku K, Nagamine M, Silva R V and Kurata R 2010 Project-based learning in graduation research program: joint development of a microscope-scale screening system

- of inhibitory drugs for amyloid aggregation *4th Int. Symp. on Advances in Technology Education (Kagoshima)* pp 246–50
- [29] Xiao L H, Zhao D, Chan W H, Choi M M F and Li H W 2010 Inhibition of beta 1–40 amyloid fibrillation with *N*-acetyl-L-cysteine capped quantum dots *Biomaterials* **31** 91–8
- [30] Xu G X, Yong K T, Roy I, Mahajan S D, Ding H, Schwartz S A and Paras N P 2008 Bioconjugated quantum rods as targeted probes for efficient transmigration across an *in vitro* blood-brain barrier *Bioconjug. Chem.* **19** 1179–85
- [31] Nazem A and Mansoori G A 2011 Nanotechnology for Alzheimer's disease detection and treatment *Insciences J.* **1** 169–93
- [32] Brambilla D, Droumaguet B L, Nicolas J, Hashemi S H, Wu L P, Moghimi S M, Couvreur P and Andrieux K 2011 Nanotechnologies for Alzheimer's disease: diagnosis, therapy, and safety issues *Nanomed. Nanotechnol.* **7** 521–40
- [33] Kaye R, Head E, Thompson J L, McIntire T M, Milton S C, Cotman C W and Glabe C G 2003 Common structure of soluble Amyloid oligomers implies common mechanism of pathogenesis *Science* **300** 486–90